

## TABLE OF CONTENTS

|                           |  |       |
|---------------------------|--|-------|
| Acknowledgements          |  | iii   |
| Abstract (English)        |  | v     |
| Abstract (Thai)           |  | vii   |
| List of Tables            |  | xvii  |
| List of Figures           |  | xviii |
| Abbreviations and Symbols |  | xxvii |
| Chapter 1                 | Introduction   |       |
|                           | 1.1 Background   | 1     |
|                           | 1.2 TiO <sub>2</sub> photocatalysts                        | 3     |
|                           | 1.2.1 Titanium dioxide                                     | 3     |
|                           | 1.2.2 Commercial TiO <sub>2</sub>                          | 6     |
|                           | 1.3 Properties of transition metal ions                    | 6     |
|                           | 1.3.1 Vanadium   | 6     |
|                           | 1.3.2 Iron   | 8     |
|                           | 1.3.3 Copper   | 10    |
|                           | 1.4 Heterogeneous photocatalysis                           | 12    |
|                           | 1.4.1 Semiconductors as photocatalysts                     | 12    |
|                           | 1.4.2 Principles of heterogeneous photocatalytic processes | 14    |
|                           | 1.4.3 Photocatalytic oxidation                             | 18    |
|                           | 1.4.4 Photocatalytic reduction                             | 19    |
|                           | 1.5 Modified photocatalysts: enhancement of                |       |

|  |    |
|--|----|
| photocatalytic activity  | 19 |
| 1.5.1 Doping with transition metal ions  | 19 |
| 1.5.2 Metal deposition   | 20 |
| 1.5.3 Coupled semiconductors   | 22 |
| 1.5.4 Application of nano-sized particles  | 22 |
| 1.6 Factor influencing photocatalytic activity   | 23 |
| 1.6.1 Extrinsic parameters   | 23 |
| 1.6.1.1 Light intensity  | 23 |
| 1.6.1.2 Temperature  | 23 |
| 1.6.1.3 Photocatalyst loading  | 24 |
| 1.6.1.4 Influence of pH  | 24 |
| 1.6.2 Intrinsic parameters   | 25 |
| 1.6.2.1 Effect of surface area on photoactivity  | 25 |
| 1.6.2.2 Effect of particle size on photoactivity   | 25 |
| 1.6.2.3 The importance of the crystal structure  | 25 |
| 1.7 Application of TiO <sub>2</sub>  | 25 |
| 1.7.1 Self-sterilizing photocatalytic  | 25 |
| 1.7.2 Self-cleaning photocatalytic of building materials<br>for indoor and outdoor application | 26 |
| 1.7.3 Anti-fogging glass   | 26 |
| 1.7.4 Photocatalytic water purification  | 26 |
| 1.8 Preparation of photocatalysts  | 27 |
| 1.8.1 Sol-gel method   | 28 |

|         |  |    |
|---------|--|----|
| 1.8.2   | Precipitation method                             | 30 |
| 1.8.3   | Solvothermal method                              | 30 |
| 1.8.4   | Microemulsion method                             | 30 |
| 1.8.5   | Combustion synthesis                             | 31 |
| 1.8.6   | Impregnation method                              | 31 |
| 1.8.7   | Hydrothermal method                              | 31 |
| 1.9     | Characterization techniques                      | 32 |
| 1.9.1   | X-ray diffraction method                         | 32 |
| 1.9.1.1 | Identification of phases by XRD                  | 33 |
| 1.9.1.2 | Particle size measurement by XRD                 | 33 |
| 1.9.2   | Surface area and porosity determination          | 35 |
| 1.9.2.1 | Surface area determination                       | 35 |
| 1.9.2.2 | Pore size distribution                           | 37 |
| 1.9.3   | Transmission electron microscopy and diffraction | 40 |
| 1.9.4   | Chemical composition analysis                    | 44 |
| 1.9.4.1 | X-ray spectroscopy in the electron microscope    | 44 |
| 1.9.4.2 | Selected-area diffraction                        | 46 |
| 1.9.4.3 | Measurement of electron diffraction patterns     | 48 |
| 1.9.5   | Scanning Electron Microscope (SEM)               | 48 |
| 1.9.5.1 | Instrumentation                                  | 49 |
| 1.9.5.2 | Interaction of electron beams with solids        | 51 |
| 1.9.6   | X-ray photoelectron spectroscopy (XPS)           | 53 |

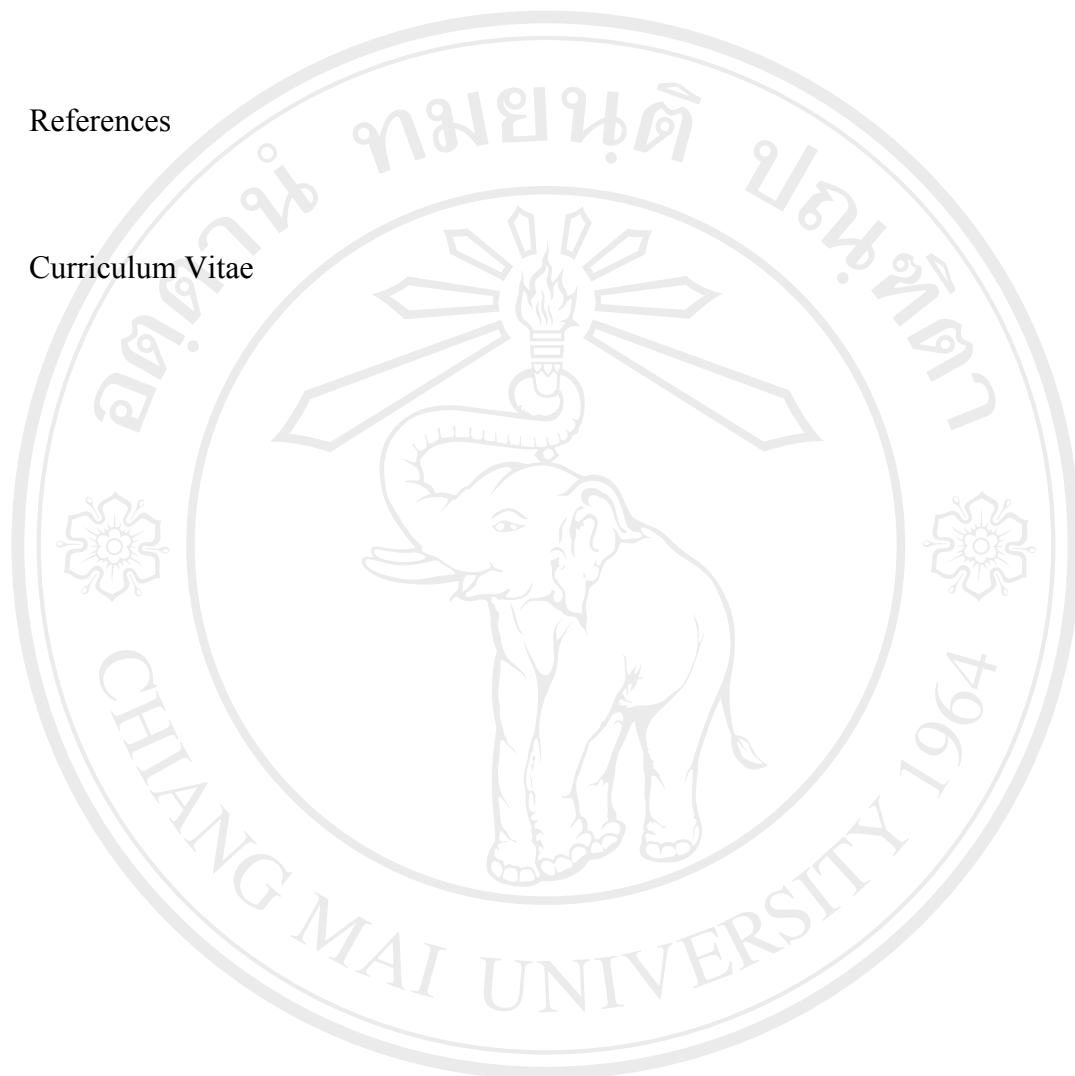
|           |  |    |
|-----------|--|----|
|           | 1.9.7 UV-Vis diffuse reflectance spectroscopy  | 56 |
|           | 1.9.8 Fourier transform infrared spectrophotometry (FT-IR)                             | 61 |
|           | 1.9.8.1 Qualitative Analysis   | 62 |
|           | 1.9.8.2 Quantitative analysis  | 62 |
|           | 1.9.8.3 Physical principles  | 63 |
|           | 1.9.8.4 Sample Preparation   | 63 |
|           | 1.10 Literature review of TiO <sub>2</sub>   | 64 |
|           | 1.11 Research objectives   | 72 |
| Chapter 2 | Experimental   |    |
|           | 2.1 Materials  | 73 |
|           | 2.2 Instruments  | 74 |
|           | 2.3 Sample preparations  | 75 |
|           | 2.3.1 The modified sol-gel method  | 75 |
|           | 2.3.1.1 Preparation of pure TiO <sub>2</sub>   | 75 |
|           | 2.3.1.2 Preparation of transition metal ions<br>(V, Cu, and Fe) doped TiO <sub>2</sub> | 76 |
|           | 2.3.2 The impregnation method  | 76 |
|           | 2.3.2.1 Preparation of Fe-doped TiO <sub>2</sub>                                       | 76 |
|           | 2.4 Sample characterization  | 77 |
|           | 2.4.1 UV-Vis diffuse reflectance spectroscopy  | 77 |
|           | 2.4.2 X-ray diffraction (XRD)  | 77 |

|           |  |     |
|-----------|--|-----|
| 2.4.3     | Transmission electron microscopy (TEM)   | 78  |
| 2.4.4     | Scanning electron microscopy (SEM)   | 78  |
| 2.4.5     | Specific surface area (BET)  | 78  |
| 2.4.6     | X-ray photoelectron spectroscopy (XPS)   | 79  |
| 2.4.7     | Fourier transform infrared spectrophotometry (FT-IR)                                 | 79  |
| 2.4.8     | Photocatalytic activity studies  | 79  |
| 2.4.8.1   | Apparatus  | 79  |
| 2.4.8.2   | Preparation of photocatalyst suspension<br>and operation                             | 81  |
| 2.4.8.3   | Calibration curve measurement  | 82  |
| Chapter 3 | Results and Discussion   |     |
| 3.1       | Preparation of pure TiO <sub>2</sub> and V, Cu, Fe-doped<br>TiO <sub>2</sub> powders | 84  |
| 3.2       | Samples characterization   | 85  |
| 3.2.1     | UV-Vis diffuse reflectance spectroscopy studies                                      | 85  |
| 3.2.2     | BET-Specific surface area studies  | 94  |
| 3.2.3     | X-ray diffraction studies  | 99  |
| 3.2.4     | Transmission electron microscopy studies   | 108 |
| 3.2.4.1   | TEM of pure TiO <sub>2</sub> prepared by<br>the modified sol-gel method              | 108 |
| 3.2.4.2   | TEM of V-doped TiO <sub>2</sub> prepared by<br>the modified sol-gel method           | 110 |

|         |   |     |
|---------|---|-----|
| 3.2.4.3 | TEM of Cu-doped TiO <sub>2</sub> prepared by<br>the modified sol-gel method                 | 112 |
| 3.2.4.4 | TEM of Fe-doped TiO <sub>2</sub> prepared by<br>the modified sol-gel method                 | 114 |
| 3.2.4.5 | TEM of Fe-doped TiO <sub>2</sub> prepared by the<br>impregnation method                     | 118 |
| 3.2.5   | Scanning electron microscopy studies  | 121 |
| 3.2.6   | X-ray photoelectron spectroscopy (XPS) studies  | 124 |
| 3.2.6.1 | XPS of pure TiO <sub>2</sub> prepared by<br>the modified sol-gel method                     | 124 |
| 3.2.6.2 | XPS of Cu-doped TiO <sub>2</sub> prepared by<br>the modified sol-gel method                 | 126 |
| 3.2.6.3 | XPS of Fe-doped TiO <sub>2</sub> prepared by<br>the modified sol-gel method                 | 128 |
| 3.2.6.4 | XPS of Fe-doped TiO <sub>2</sub> prepared by the<br>impregnation method                     | 130 |
| 3.3     | Photocatalytic activity studies using UNSW's spiral<br>photoreactor                         | 132 |
| 3.3.1   | Calibration curve   | 132 |
| 3.3.2   | Photocatalytic activity of pure TiO <sub>2</sub> prepared by<br>the modified sol-gel method | 133 |
| 3.3.3   | Photocatalytic activity of V, Cu, Fe-doped TiO <sub>2</sub><br>with oxalic acid             | 135 |

|           |  |     |
|-----------|--|-----|
| 3.3.4     | Photocatalytic activity of V, Cu, Fe-doped TiO <sub>2</sub><br>with various organic compounds under UVA,<br>solar light, and visible light irradiation | 139 |
| 3.4       | Photocatalytic activity studies using CMU's spiral<br>photoreactor   | 146 |
| 3.4.1     | Calibration curve  | 147 |
| 3.4.2     | Photocatalytic activity of Fe-doped TiO <sub>2</sub><br>prepared by the impregnation method  | 148 |
| 3.4.2.1   | Photocatalytic activity of Fe-doped TiO <sub>2</sub><br>with oxalic acid under UVA, solar light,<br>and visible light irradiation                      | 148 |
| 3.4.2.2   | Photocatalytic activity of Fe-doped TiO <sub>2</sub> with<br>various organic compounds under UVA,<br>solar light, and visible light irradiation        | 150 |
| 3.5       | Fourier transform infrared spectrophotometry studies   | 153 |
| Chapter 4 | Conclusions  |     |
| 4.1       | Synthesis and characterization of pure TiO <sub>2</sub><br>and V, Cu, Fe-doped TiO <sub>2</sub> by the modified<br>sol-gel method                      | 165 |
| 4.2       | Photocatalytic activity of pure TiO <sub>2</sub><br>and V, Cu, Fe-doped TiO <sub>2</sub> by the modified<br>sol-gel method                             | 168 |

|     |                             |     |
|-----|-----------------------------|-----|
| 4.3 | Suggestions for future work | 169 |
|     | References                  | 171 |
|     | Curriculum Vitae            | 188 |



ลิขสิทธิ์มหาวิทยาลัยเชียงใหม่

**LIST OF TABLES**

| <b>Table</b> |   | <b>Page</b> |
|--------------|---|-------------|
| 1.1          | Types and physical properties of titanium dioxide | 5           |
| 1.2          | Chemical and physical properties of titanium      | 6           |
| 1.3          | Chemical and physical properties of vanadium      | 8           |
| 1.4          | Chemical and physical properties of iron          | 10          |



|     |  |     |
|-----|--|-----|
| 1.5 | Chemical and physical properties of copper   | 12  |
| 1.6 | Environmental applications of TiO <sub>2</sub> photocatalysis  | 27  |
| 3.1 | Relation between elements and atomic% of V-doped TiO <sub>2</sub>  | 111 |
| 3.2 | Relation between elements and atomic% of Fe-doped TiO <sub>2</sub>   | 117 |
| 3.3 | Relation between elements and atomic% of Fe-doped TiO <sub>2</sub> prepared by the impregnation method                     | 121 |
| 3.4 | XPS binding energies (eV) of pure TiO <sub>2</sub> , 2 at.% Fe-doped TiO <sub>2</sub> , 0.5 at.% Cu-doped TiO <sub>2</sub> | 124 |
| 3.5 | Calibration data of different concentrations of sucrose  | 132 |
| 3.6 | Calibration data of different concentrations of sucrose  | 138 |
| 3.7 | FT-IR absorption bands of oxalic acid and formic acid  | 159 |

## LIST OF FIGURES

| Figure |   | Page |
|--------|---|------|
| 1.1    | The structure of titanium dioxide in anatase phase              | 4    |
| 1.2    | The structure of titanium dioxide in rutile phase               | 4    |
| 1.3    | The structure of titanium dioxide in brookite phase             | 5    |
| 1.4    | Energy band diagrams for metallic, semiconductor, and insulator | 14   |
| 1.5    | Energy structures of various photoconductors                    | 15   |

|      |   |    |
|------|---|----|
| 1.6  | Simplified diagram of the mechanism for activation of semiconductor photocatalyst   | 16 |
| 1.7  | Electron mediation by metal ion in contact with TiO <sub>2</sub> surface  | 21 |
| 1.8  | Schematic diagram of X-ray line broadening effects  | 34 |
| 1.9  | Typical isotherm for N <sub>2</sub> adsorption-desorption on $\gamma$ -Al <sub>2</sub> O <sub>3</sub>   | 35 |
| 1.10 | BET plot for surface area (S.A.) determination for $\gamma$ -Al <sub>2</sub> O <sub>3</sub>   | 36 |
| 1.11 | BJH analysis of data from Figure 1.10 showing differential and cumulative mesopore volume distributions for $\gamma$ -Al <sub>2</sub> O <sub>3</sub>  | 39 |
| 1.12 | (a) Signals generated during electron beam-sample interactions; (b) a 'ray diagram' of image formation; and (c) a schematic diagram of the principles of electron microscopy: (A) imaging and (B) diffraction | 43 |
| 1.13 | The process of electron-stimulated X-ray emission in the electron microscope  | 44 |

|               |             |
|---------------|-------------|
| <b>Figure</b> | <b>Page</b> |
|---------------|-------------|

|      |   |    |
|------|---|----|
| 1.14 | (a) Ray diagram showing the formation of the diffraction pattern and intermediate image by the objective lens. (b) In a three-lens microscope the intermediate lens (or projector 1) is normally focused on the intermediate image formed by objective lens | 47 |
| 1.15 | Schematic diagram of scanning electron microscope with CRT display  | 51 |
| 1.16 | Diffuse reflectance spectrum of the fundamental absorption edge of  |    |

titanium dioxide powder. Absorbance ( $(F(R_\infty))$ ) vs. wavelength:

(i) indirect transition; (ii) direct transition; (iii) direct band gap;

$$E_g = hc / \lambda_g \quad 58$$

- 1.17 (a) Schematic energy band diagram showing hole-electron pair formation as a consequence of differing energies of incident radiation; (b) schematic energy band diagram (energy vs. wave vector  $\tilde{k}$ ) illustrating the difference between direct and indirect transitions 60
- 2.1 Schematic of the modified sol-gel method 75
- 2.2 Schematic of spiral photoreactor 81
- 3.1 UV-Vis (a) reflection spectra, (b) absorbance Kubelka-Munk, and (c) relation between band gap energy and  $[F(R)h\nu]^{1/2}$  of P25, pure TiO<sub>2</sub> and 0.1-2 at.% of V-doped TiO<sub>2</sub> 87

| <b>Figure</b>  | <b>Page</b> |
|--|-------------|
| 3.2 UV-Vis (a) reflection spectra, (b) absorbance Kubelka-Munk, and (c) relation between band gap energy and $[F(R)h\nu]^{1/2}$ of P25, pure TiO <sub>2</sub> and 0.5-5 at.% of Cu-doped TiO <sub>2</sub>  | 89          |
| 3.3 UV-Vis (a) reflection spectra, (b) absorbance Kubelka-Munk, and (c) relation between band gap energy and $[F(R)h\nu]^{1/2}$ of P25, pure TiO <sub>2</sub> and 0.1-10 at.% of Fe-doped TiO <sub>2</sub> prepared by the modified sol-gel method | 90          |

|               |   |             |
|---------------|---|-------------|
| 3.4           | UV-Vis (a) reflection spectra, (b) absorbance Kubelka-Munk, and (c) relation between band gap energy and $[F(R)h\nu]^{1/2}$ of P25, pure TiO <sub>2</sub> and 1-5 at.% of Fe-doped TiO <sub>2</sub> prepared by the impregnation method | 92          |
| 3.5           | SSA and BET equivalent diameter of pure TiO <sub>2</sub> at different calcination temperatures of 400-600 °C for 3h   | 95          |
| 3.6           | SSA and BET equivalent diameter of 0.1-2 at.% of V-doped TiO <sub>2</sub> prepared by the modified sol-gel method   | 97          |
| 3.7           | SSA and BET equivalent diameter of 0.5-5 at.% of Cu-doped TiO <sub>2</sub> prepared by the modified sol-gel method  | 98          |
| 3.8           | SSA and BET equivalent diameter of 0.1-10 at.% of Fe-doped TiO <sub>2</sub> prepared by the modified sol-gel method   | 99          |
| <b>Figure</b> |   | <b>Page</b> |
| 3.9           | SSA and BET equivalent diameter of 1-5 at.% of Fe-doped TiO <sub>2</sub> prepared by the impregnation method  | 99          |
| 3.10          | XRD patterns of pure TiO <sub>2</sub> prepared by the modified sol-gel method and subjected to heat treatment between 400-900 °C for 3h   | 101         |
| 3.11          | Effect of calcination temperature on phase composition and particle size TiO <sub>2</sub> prepared by the modified sol-gel method and subjected to heat treatment between 400-900 °C for 3h   | 102         |
| 3.12          | XRD patterns of 0.1-2 at.% of V-doped TiO <sub>2</sub> prepared by the modified sol-gel method at the calcination temperature of 400 °C for 3h  | 104         |

|      |  |     |
|------|--|-----|
| 3.13 | XRD patterns of 0.5-5 at.% of Cu-doped TiO <sub>2</sub> prepared by the modified sol-gel method at the calcination temperature of 400 °C for 3h  | 105 |
| 3.14 | XRD patterns of and 0.1-10 at.% of Fe-doped TiO <sub>2</sub> prepared by the modified sol-gel method at the calcination temperature of 400 °C for 3h   | 106 |
| 3.15 | XRD patterns of 1-5 at.% of Fe-doped TiO <sub>2</sub> prepared by impregnation method at the calcination temperature of 400 °C for 3h  | 107 |
| 3.16 | TEM images of pure TiO <sub>2</sub> prepared by the modified sol-gel method and subjected to heat treatment at (a) 400 °C (b) 500 °C (c) 600 °C (d) 700 °C for 3h, respectively. Insets show the corresponding diffraction patterns of pure TiO <sub>2</sub> . | 109 |

| <b>Figure</b> | <b>Page</b>   |     |
|---------------|---|-----|
| 3.17          | TEM micrographs of (a) 0.1 at.% of V, and (b) 0.5 at.% of V-doped TiO <sub>2</sub> prepared by the modified sol-gel method. The square areas selected emphasized for the EDS investigation with chemical elements of V-doped TiO <sub>2</sub> . | 111 |
| 3.18          | EDS analysis of (a) 0.1 at.% of V and (b) 0.5 at.% of V-doped TiO <sub>2</sub>  | 111 |
| 3.19          | TEM micrographs of (a) 0.5 at% of Cu, (b) 1 at% of Cu, and (c) 2 at% of Cu-doped TiO <sub>2</sub> prepared by the modified sol-gel method   | 113 |
| 3.20          | TEM micrographs of (a) 0.5 at.% of Fe, (b) 1 at.% of Fe, (c) 2 at.% of Fe, and (d) 5 at.% of Fe-doped TiO <sub>2</sub> prepared by the modified sol-gel method. The square areas selected emphasized for the EDS                                |     |

|               |   |             |
|---------------|---|-------------|
|               | investigation with chemical elements of Fe-doped TiO <sub>2</sub> .   | 115         |
| 3.21          | EDS analysis of (a) 0.5 at.% of Fe, (b) 1 at.% of Fe, (c) 2 at.% of Fe, and (d) 5 at.% of Fe-doped TiO <sub>2</sub>   | 117         |
| 3.22          | TEM micrographs of (a) 1 at% of Fe, (b) 2 at% of Fe, (c) 3 at% of Fe, (d) 4 at% of Fe, and (e) 5 at% of Fe-doped TiO <sub>2</sub> prepared by the impregnation method. The square areas selected emphasized for the EDS investigation with chemical elements of Fe-doped TiO <sub>2</sub> . | 119         |
| 3.23          | EDS analysis of (a) 2 at.% of Fe, (b) 3 at.% of Fe, (c) 4 at.% of Fe, (d) 5 at.% of Fe-doped TiO <sub>2</sub>   | 120         |
| 3.24          | (a) SEM micrograph and EDS mapping mode of 0.5 at.% Cu-doped TiO <sub>2</sub> (b) Ti, (c) O, and (c) Cu elements  | 123         |
| <b>Figure</b> |   | <b>Page</b> |
| 3.25          | XPS spectra of pure TiO <sub>2</sub> (a) survey, (b) Ti 2p peaks, and (c) O 1s peaks  | 125         |
| 3.26          | XPS spectra of 0.5 at.% of Cu-doped TiO <sub>2</sub> (a) survey, (b) Ti 2p peaks, and (c) O 1s  | 128         |
| 3.27          | XPS spectra of 2 at.% of Fe-doped TiO <sub>2</sub> (a) survey, (b) Ti 2p peaks, (c) O 1s, and (d) Fe 2p peaks   | 129         |
| 3.28          | XPS spectra of pure TiO <sub>2</sub> and 2 at.% of Fe-doped TiO <sub>2</sub> prepared by impregnation method (a) survey, (b) Ti 2p peaks, (c) O 1s, and (d) Fe 2p peaks   | 131         |
| 3.29          | Calibration slope for conductivity probe  | 133         |
| 3.30          | The rate of 50% mineralization rate of oxalic acid with 500 µg of carbon by Degussa P25 (as a reference) and TiO <sub>2</sub> at different calcination temperature  |             |

|               |   |             |
|---------------|---|-------------|
|               | 400-700 °C for 3h under UVA irradiation   | 134         |
| 3.31          | The rate of 50% mineralization of oxalic acid with 500 µg of carbon by using 0.1-2 at.% of V-doped TiO <sub>2</sub> under UVA irradiation   | 136         |
| 3.32          | The rate of 50% mineralization of oxalic acid with 500 µg of carbon by using 0.1-10 at.% Fe-doped TiO <sub>2</sub> under UVA irradiation  | 136         |
| 3.33          | The rate of 50% mineralization of oxalic acid with 500 µg of carbon by using 0.05-5 at.% Cu-doped TiO <sub>2</sub> under UVA irradiation  | 137         |
| 3.34          | Percent mineralization of oxalic acid with 500 µg of carbon using Degussa P25, pure TiO <sub>2</sub> , and 0.1-2 at.% of V-doped TiO <sub>2</sub> under visible light and irradiation time of 180 minutes | 137         |
| <b>Figure</b> |   | <b>Page</b> |
| 3.35          | Percent mineralization of oxalic acid with 500 µg of carbon using Degussa P25, pure TiO <sub>2</sub> , and 0.5-5 at% of Cu-doped TiO <sub>2</sub> under visible light and irradiation time of 180 min     | 138         |
| 3.36          | Percent mineralization of oxalic acid with 500 µg of carbon using Degussa P25, pure TiO <sub>2</sub> , and 0.1-10 at% of Fe-doped TiO <sub>2</sub> under visible light and irradiation time of 90 min     | 139         |
| 3.37          | The rate of 50% mineralization of sucrose, phenol, oxalic acid, formic acid, methanol, and malonic acid with 500 µg of carbon by various photocatalysts under UVA irradiation                             | 140         |
| 3.38          | The rate of 50% mineralization of sucrose, phenol, oxalic acid, formic acid, methanol, and malonic acid with 500 µg of carbon by using various photocatalysts under solar light irradiation               | 141         |

|               |   |             |
|---------------|---|-------------|
| 3.39          | Mineralization of sucrose, phenol, oxalic acid, formic acid, methanol, and malonic acid with 500 $\mu\text{g}$ of carbon by using various photocatalysts under visible light illumination (fixed irradiation time = 3h, except 2 at.% of Fe doped $\text{TiO}_2$ fixed irradiation time = 90 min for oxalic acid) | 142         |
| 3.40          | Calibration slope for conductivity probe  | 148         |
| 3.41          | The rate of 50% mineralization of oxalic acid with 500 $\mu\text{g}$ of carbon by using 1-5 at.% of Fe-doped $\text{TiO}_2$ under UVA irradiation as compared to P25 and pure $\text{TiO}_2$  | 150         |
| <b>Figure</b> |   | <b>Page</b> |
| 3.42          | The rate of 50% mineralization of oxalic acid with 500 $\mu\text{g}$ of carbon by using 1-5 at.% of Fe-doped $\text{TiO}_2$ under solar light irradiation as compared to P25 and pure $\text{TiO}_2$  | 150         |
| 3.43          | Mineralization of oxalic acid with 500 $\mu\text{g}$ of carbon by using various amount of Fe doping under visible light illumination fixed irradiation time = 50 min as compared to P25 and pure $\text{TiO}_2$   | 151         |
| 3.44          | The rate of 50% mineralization of sucrose, phenol, oxalic acid, formic acid, and methanol with 500 $\mu\text{g}$ of carbon by using various photocatalysts under UVA irradiation  | 152         |
| 3.45          | The rate of 50% mineralization of sucrose, phenol, oxalic acid, formic acid, and methanol with 500 $\mu\text{g}$ of carbon by using various photocatalysts under solar light irradiation  | 153         |
| 3.46          | Mineralization of sucrose, phenol, oxalic acid, formic acid, and methanol   |             |



|               |   |             |
|---------------|---|-------------|
|               | with 500 $\mu\text{g}$ of carbon by using various photocatalysts under visible light illumination (fixed irradiation time = 3h, except 2 at.% of Fe-doped $\text{TiO}_2$ fixed irradiation time = 50 min for oxalic acid)   | 154         |
| 3.47          | FT-IR spectra of (a) pure $\text{TiO}_2$ , (b) 2 at.% of Fe-doped $\text{TiO}_2$ (the modified sol-gel method, (c) 2 at.% of Fe-doped $\text{TiO}_2$ with formic acid, (d) 2 at.% of Fe-doped $\text{TiO}_2$ with oxalic acid after mineralization under visible light for 15 min, (e) formic acid, and (f) oxalic acid | 160         |
| <b>Figure</b> |   | <b>Page</b> |
| 3.48          | FT-IR spectra of (a) pure $\text{TiO}_2$ , (b) 2 at.% of Fe-doped $\text{TiO}_2$ (the impregnation method, (c) 2 at.% of Fe-doped $\text{TiO}_2$ with formic acid, (d) 2 at.% of Fe-doped $\text{TiO}_2$ with oxalic acid after mineralization under visible light for 15 min, (e) formic acid, and (f) oxalic acid     | 161         |
| 3.49          | FT-IR spectra of (a) pure $\text{TiO}_2$ , (b) 0.5 at.% of Cu-doped $\text{TiO}_2$ , (c) 0.5 at.% of Cu-doped $\text{TiO}_2$ with formic acid, (d) 0.5 at.% of Cu-doped $\text{TiO}_2$ with oxalic acid after mineralization under visible light for 15 min, (e) formic acid, and (f) oxalic acid                       | 162         |

### ABBREVIATIONS AND SYMBOLS

|                              |   |
|------------------------------|---|
| A                            | Absorption  |
| A <sup>+</sup>               | Electron acceptor                                     |
| at. %                        | Atomic %  |
| B                            | Peak width measured at half height measured in radius |
| BET                          | Brunauer-Emmett-Teller                                |
| C                            | Amount of carbon                                      |
| C                            | A constant, related to the free energy of adsorption  |
| c                            | Speed of light  |
| CRT                          | Cathode-ray tube                                      |
| CMU                          | Chiang Mai University                                 |
| C <sub>A</sub>               | Concentration of element A                            |
| C <sub>B</sub>               | Concentration of element B                            |
| °C                           | Degrees Celsius                                       |
| d <sub>hkl</sub>             | Interplanar distance between (hkl) planes             |
| d                            | Lattice planar spacing                                |
| cb                           | Conduction band                                       |
| e <sup>-</sup>               | Electron  |
| e <sup>-</sup> <sub>cb</sub> | Conduction band electron                              |
| eV                           | Electron volt   |

|                   |   |
|-------------------|---|
| $E$               | Binding energy  |
| EDS, EDX          | Energy dispersive X-ray spectroscopy                          |
| EM                | Electron microscope   |
| $E_0$             | Energy of ground state  |
| $E_1$             | Energy of first excited state                                 |
| $E_a$             | Apparent activation energy                                    |
| $E_b$             | Binding energy  |
| $E_g$             | Optical band gap of the semiconductor                         |
| $E_k$             | Kinetic energy  |
| $E_{vac}$         | Energy of vacuum level  |
| g/L               | grams/liter   |
| $h$               | Plank's constant ( $6.63 \times 10^{-34}$ Js)                 |
| $h\nu$            | Photon energy   |
| $h^+$             | Hole  |
| $h^+_{vb}$        | Valence band hole   |
| $I_0$             | Intensity of the incident beam                                |
| $I$               | Intensity of the transmittance                                |
| $I_A$             | Background subtracted peak intensities for A                  |
| $I_B$             | Background subtracted peak intensities for B                  |
| IUPAC             | International union of pure and applied chemistry             |
| $J$               | Intensity of the reflected radiation                          |
| JCPDS             | Joint committee powder diffraction standards                  |
| K                 | Kelvin  |
| $K$               | Absorption coefficient  |
| $k$               | Conductivity value  |
| keV               | kilo electron volt  |
| kV                | kilo-volt   |
| $\tilde{k}$       | Wave vector   |
| $\tilde{k}'_{cb}$ | Wave vector of the lowest energy state in the conduction band |

|                   |   |
|-------------------|---|
| $\tilde{k}'_{vb}$ | Wave vector of the highest energy state in the valence band             |
| mg                | Milligram   |
| min               | Minute  |
| ml                | Milliliter  |
| mS                | Millisiemen   |
| n                 | Order of diffraction  |
| nm                | Nanometer ( $10^{-9}$ m)  |
| $N_a$             | Avogadro's number ( $6.02 \times 10^{23}$ )                             |
| O                 | Oxygen  |
| $O_2^{\bullet -}$ | Superoxide radical  |
| $OH^{\bullet}$    | Hydroxyl radical  |
| $P$               | Pressure at the constant temperature                                    |
| $P_0$             | Saturation pressure at the measurement temperature                      |
| $R_\alpha$        | Absolute remittance   |
| rpm               | Revolution per minute   |
| $r_k$             | Kelvin radius   |
| $r_p$             | Actual pore radius  |
| $S$               | Twice the scattering coefficient of sample                              |
| SEM               | Scanning electron microscopy  |
| SSA               | Specific surface area   |
| S.A.              | Surface area  |
| $S_{BET}$         | BET surface area  |
| $T$               | Transmittance   |
| TTIP              | Titanium tetraisopropoxide  |
| TEM               | Transmission electron microscopy  |
| $t$               | Thickness ( $t$ ) of adsorbed $N_2$ layers                              |
| $t_{hkl}$         | Particle size measured from X-rays diffracted from the ( $hkl$ ) planes |
| UNSW              | University of New South Wales   |

|                  |   |
|------------------|---|
| UV-Vis           | Ultraviolet-visible   |
| UV-Vis DRS       | Ultraviolet-visible diffuse reflectance spectroscopy  |
| $V$              | Volume, reduced to standard conditions (STP) of gas adsorbed per unit mass of adsorbent at a given pressure               |
| vb               | Valence band  |
| $V_m$            | Volume of gas adsorbed at STP per unit mass of adsorbent, when the surface is covered by a unimolecule layer of adsorbate |
| $V_{mol}$        | Molar volume of adsorbate gas at STP ( $22.4 \text{ mol}^{-1}$ )  |
| WDS              | Wavelength dispersive X-ray spectroscopy  |
| XPS              | X-ray photoelectron spectroscopy  |
| XRD              | X-ray diffraction   |
| Z                | Atomic number   |
| $\lambda$        | Wavelength  |
| $\mu\text{g}$    | Microgram ( $10^{-6} \text{ g}$ )   |
| $\mu\text{g C}$  | Microgram of carbon   |
| $\mu\text{m}$    | Micron ( $10^{-6} \text{ meter}$ )  |
| $\mu\text{S/cm}$ | MicroSiemens /square centimeter   |
| $\Phi$           | Work function   |
| $\varepsilon$    | Absorptivity  |
| $\theta$         | Bragg angle for the reflection  |
| $\nu$            | Frequency   |
| $\nu_{as}$       | Frequency asymmetric  |
| $\nu_s$          | Frequency symmetric   |